
Research Article: New Research | Cognition and Behavior

First person virtual embodiment modulates cortical network that encodes the bodily self and its surrounding space during the experience of domestic violence

<https://doi.org/10.1523/ENEURO.0263-19.2019>

Cite as: eNeuro 2020; 10.1523/ENEURO.0263-19.2019

Received: 7 July 2019

Revised: 16 November 2019

Accepted: 17 December 2019

This Early Release article has been peer-reviewed and accepted, but has not been through the composition and copyediting processes. The final version may differ slightly in style or formatting and will contain links to any extended data.

Alerts: Sign up at www.eneuro.org/alerts to receive customized email alerts when the fully formatted version of this article is published.

Copyright © 2020 de Borst et al.

This is an open-access article distributed under the terms of the Creative Commons Attribution 4.0 International license, which permits unrestricted use, distribution and reproduction in any medium provided that the original work is properly attributed.

1 **Title:** First person virtual embodiment modulates cortical network that encodes the
2 bodily self and its surrounding space during the experience of domestic violence
3 **Short title:** First person embodiment modulates personal space network
4 **Authors & Affiliations:** Aline W. de Borst^a, Maria V. Sanchez-Vives^{b,c}, Mel Slater^{d,e} &
5 Beatrice de Gelder^{e,f}
6 a. UCL Interaction Centre, University College London, London, UK.
7 b. Institut d'Investigacions Biomèdiques August Pi i Sunyer (IDIBAPS), Barcelona, Spain.
8 c. ICREA, Barcelona, Spain.
9 d. Event Lab, Department of Clinical Psychology and Psychobiology, University of
10 Barcelona, Barcelona, Spain.
11 e. Department of Computer Science, University College London, London, UK.
12 f. Brain and Emotion lab, Department of Cognitive Neuroscience, Faculty of Psychology
13 and Neuroscience, Maastricht University, the Netherlands
14 **4. Contributions:** AB, MSV, MS, BG designed research, AB performed research and
15 analyzed data, AB, MSV, MS, BG wrote paper.
16 **5. Correspondence should be addressed to:** A.W. de Borst, 66-72 Gower Street, WC1E
17 6AA, London, UK, a.deborst@ucl.ac.uk
18 **6. Number of Figures:** 7
19 **7. Number of Tables:** 1
20 **8. Number of Multimedia:** 0
21 **9. Number of words for abstract:** 249
22 **10. Number of words for significance statement:** 102
23 **11. Number of words for introduction:** 743
24 **12. Number of words for Discussion:** 1862
25 **13. Acknowledgements:** We would like to thank Guillermo Iruretagoyena, Xavi Navarro,
26 Sofía Seinfeld, and Chris Wiggins for their help with the VR stimuli and set-up and
27 Giancarlo Valente and Jukka-Pekka Kauppi for their suggestions on the ISC analyses. This
28 work was supported by FP7/2007-2013, ERC grant agreement number 295673.
29 **14. Conflict of Interest:** Authors report no conflict of interest
30 **15. Funding sources:** This work was supported by FP7/2007-2013, ERC grant agreement
31 number 295673.
32

33 **First person virtual embodiment modulates cortical network that encodes the bodily self and its**
34 **surrounding space during the experience of domestic violence**

35

36 **Abstract**

37 Social aggression, such as domestic violence, has been associated with a reduced ability to take on
38 others' perspectives. In this naturalistic imaging study, we investigated whether training human
39 participants to take on a first person embodied perspective during the experience of domestic violence
40 enhances the identification with the victim and elicits brain activity associated with the monitoring of
41 the body and surrounding space and the experience of threat. We combined fMRI measurements with
42 preceding virtual reality exposure from either first or third person perspective to manipulate whether
43 domestic abuse was perceived as directed to oneself or another. We found that first person perspective
44 exposure increased body ownership and identification with the virtual victim. Furthermore, when the
45 stimulus was perceived as directed towards oneself, the brain network that encodes the bodily self and
46 its surrounding space was more strongly synchronized across participants and connectivity increased
47 from premotor and intraparietal cortex towards superior parietal lobe. Additionally, when the stimulus
48 came near the body, brain activity in the amygdala strongly synchronized across participants. Exposure
49 to third person perspective reduced synchronization of brain activity in the personal space network,
50 increased modulation of visual areas and strengthened functional connectivity between premotor
51 cortex, supramarginal gyrus and primary visual cortex. In conclusion, our results suggest that first person
52 perspective embodiment training enhances experience from the viewpoint of the virtual victim, which is
53 accompanied by synchronization in the fronto-parietal network to predict actions towards the body and
54 in the amygdala to signal the proximity of the stimulus.

55

56 **Significance Statement**

57 Using a combination of virtual reality and fMRI, our work reveals how first person perspective
58 embodiment increases identification with the virtual victim during the experience of domestic abuse.
59 We showed that when participants are embodied in the virtual victim the fronto-parietal brain network
60 responsible for the representation of the bodily self and its surrounding space showed highly
61 synchronized activity across participants when experiencing domestic abuse. Moreover, in this condition
62 proximity of the aggressor strongly correlated with neural synchronization of the amygdala. We
63 conclude that first person perspective embodiment allows participants to identify with the virtual victim
64 through changes in this fronto-parietal network.

65

66 **Introduction**

67 Perspective taking enhances the ability to understand another person's actions, thoughts and emotions.

68 In cases where it is more difficult to visualize the other's viewpoint specific training can be used to

69 support perspective taking. In the virtual body ownership illusion, multisensory feedback, often

70 combined with a first person perspective, is used to create the illusion that a virtual body is part of the

71 own body (Kokkinara and Slater, 2014). First person perspective and the sense of ownership over one's

72 own body or an artificial body is supported by multisensory integration in the brain, where regions, such

73 as the ventral premotor cortex (vPM), intraparietal sulcus (IPS), primary somatosensory cortex (PSC) and

74 temporoparietal cortex, integrate information from different sensory modalities (Blanke, 2012; Ehrsson,

75 2012; Serino, 2019). These brain regions are thought to not only integrate information from the body,

76 but also from the space directly surrounding the body; the peripersonal space (Rizzolatti et al., 1981).

77 Research has shown that even when the virtual body has a different age, gender or race, the body

78 ownership illusion leads people to take on the perspective and characteristics of the virtual character

79 (Banakou et al., 2013; Hamilton-Giachritsis et al., 2018). This type of training has also been utilized in

80 individuals with a reduced ability to take on others' perspectives, such as violent offenders (Seinfeld et

81 al., 2018). The peripersonal space can also be modulated by this illusion, such that actions in the space

82 surrounding the artificial body are perceived as if they were close to the real body (Ehrsson et al., 2007).

83 Here, we investigated how the brain allows for these changes in perspective, as this could form the basis

84 for understanding how behavioral change in offenders could be supported through embodiment

85 training. In specific, we studied whether taking on the viewpoint of a victim of domestic abuse increases

86 activity in brain regions responsive to threat and protection of the body.

87

88 A vast body of literature has documented animal and human threat processing networks in the brain,

89 which include subcortical structures, such as the amygdala, and the visuo-motor cortex for sensory

90 detection and preparatory responses (LeDoux, 2003; Han et al., 2008). For fast decision making on
91 whether to defend against a potential threat it is vital to integrate information in nearby space across
92 the different senses (Pereira and Moita, 2016). Recent animal studies have shown that different neural
93 circuits mediate fear responses according to the nature and proximity of the threat (Silva et al., 2016).
94 However, in humans threat has been mainly investigated with static images (Fernandes et al., 2016;
95 Sussman et al., 2016), which contrasts with the relevance of movement in the perception of threat
96 (Mobbs et al., 2010; Ahs et al., 2015). In this exploratory study, we used a naturalistic approach to
97 investigate the neural correlates of perspective taking during threat. To this end we utilized virtual
98 reality (VR), as this typically creates the perceptual illusion of ‘presence’ and ‘plausibility’ (Slater, 2009),
99 which, together with first person perspective and body ownership, typically lead participants to behave
100 similarly in VR to how they would behave in reality (Banakou et al., 2013; Maister et al., 2015). The
101 experimental design of this fMRI study follows earlier investigations using free viewing of natural scenes
102 (Bartels and Zeki, 2004; Hasson et al., 2004), rather than repeated presentation of short static stimuli, in
103 order to make the experience as realistic as possible. This approach does not allow for the use of
104 conventional general linear model (GLM) analyses, as conditions are not repeated multiple times.
105 Instead, we calculated the synchrony of brain activity across participants using intersubject correlation
106 (ISC; Hasson et al., 2004), which allows for the analysis of brain responses without a-priori definition of
107 the stimulus design. In order to control for all lower level stimulus properties between the two
108 conditions, we presented the participants with an identical 3D threat scenario during fMRI
109 measurements in both conditions, with differences between conditions induced by a preceding first or
110 third person perspective VR exposure. We hypothesized that when the observer is primed to inhabit the
111 space of the virtual victim information is transmitted from the visual and auditory regions to the
112 multisensory integration areas in the vPM and IPS, where brain activity will be more strongly
113 synchronized across participants. We also expected stronger synchronization of brain activity in threat

114 processing regions, such as the amygdala, during first person perspective experience of nearby threat, as

115 the threat would be perceived to come close to the body.

116

117 **Materials and Methods**

118 **Participants**

119 Twenty healthy volunteers participated in this study. Half of the participants were male (mean age 22.3
120 years; range 19-28) and half were female (mean age 20.3 years; range 18-24). All participants had
121 normal or corrected-to-normal vision and gave their informed consent. Exclusion criteria were the
122 institute's MRI safety criteria. Due to the nature of the stimuli, we also excluded volunteers who had a
123 criminal record, or a history of physical or emotional abuse. The study was approved by the local ethical
124 committee.

125

126 **Stimuli and materials**

127 The stimuli consisted of a VR scenario, two auditory stimuli containing instructions, and one 3D split-
128 screen video. The VR scenario displayed a female avatar in the hallway of a house (see Fig. 1, left). There
129 were two mirrors in the hallway, two doors on opposite ends, and a sideboard. The scenario could be
130 viewed from a first person perspective (1PP), or a third person perspective (3PP). The VR environment
131 was built in Unity (Unity Technologies, San Francisco, USA). The participants viewed the VR scenario
132 using an Oculus Rift DK2 (Oculus VR, Menlo Park, USA), which is a head-mounted display especially
133 designed to view VR. The Oculus Rift has an OLED display with a 960 x 1080 resolution per eye, and uses
134 an infrared camera for positional tracking of the headset. Stereoscopic vision was obtained by projecting
135 the stimulus in a slightly different angle to the left and right eye. Each of the auditory stimuli lasted 2:08
136 min and consisted of a female voice giving instructions for several visuomotor exercises in the VR
137 scenario from either the first person or the third person perspective (e.g. "move your head to the right
138 until you see the edge of the mirror"). The 3D split-screen video shown in the MRI scanner was a
139 recording of a VR domestic abuse scenario from first person perspective (Fig. 1, right). In this abuse
140 scenario, a male avatar entered the hallway from one of the doors and started addressing the female

141 avatar in a demeaning and aggressive manner. Over the course of 2:37 min, the male avatar throws the
142 phone through the hallway and approaches the female closely while continuing to verbally abuse her.
143 The 3D video was viewed inside the MRI scanner using VisStim MRI-compatible goggles (Resonance
144 Technology, Northridge, USA). The VisStim goggles contain two displays, each with a 600 x 800
145 resolution, set within a rubber head mount. Similar to the Oculus Rift, stereoscopic vision was obtained
146 by projecting the split-screen video onto the two screens. A VR questionnaire consisting of 17 items
147 relating to different aspects of the VR experience was used to assess embodiment.

148

149 **Experimental procedure**

150 The experiment consisted of two different sessions, which were one week apart. In the first session,
151 participants were informed about the study and signed the informed consent form. Afterwards, the
152 participants were familiarized with the MRI environment. Subsequently, outside of the scanner room,
153 they put on the Oculus Rift and followed auditory instructions to perform several visuomotor exercises.
154 They saw the VR scenario from either the first-person perspective or the third-person perspective
155 (counterbalanced). In the first person perspective (1PP session) they looked into a full length mirror and
156 saw the female avatar performing head movements that were consistent with the participants' own
157 movements. The synchrony between the female avatars' movements and the participants' own
158 movements contributes to the illusion of body ownership (Banakou and Slater, 2014) (Fig. 1, top left). In
159 the third person perspective scenario (3PP session), the participants performed the same movements as
160 indicated by the auditory instructions, but instead they viewed the mirror and female avatar from a
161 slight distance. In this perspective, the virtual camera viewpoint, rather than the female avatar, moved
162 consistently with the participants' head movements. The participants did not have a virtual body and
163 therefore the visuomotor exercises could not contribute to the body ownership illusion (Fig. 1, bottom
164 left). During the VR exercises the participants were not exposed to the virtual threat. After the first

165 person or third person visuomotor exercises with the Oculus, the participants were blindfolded (in order
 166 to maintain the 1PP or 3PP illusion) and led to the MRI scanner. During fMRI measurements the
 167 participants passively viewed a 3D video of the VR environment where they, from the perspective of the
 168 female character, were verbally and psychologically abused by an approaching male character (Fig. 1,
 169 right). The 3D video shown during fMRI measurements was identical in both sessions. After the fMRI
 170 measurements participants filled out the VR questionnaire. At the end of the first session participants
 171 were partially debriefed about the study, were asked about how they experienced the scenario and if
 172 they were affected by it. Moreover, they were asked to contact the experimenter if they had any
 173 reoccurring thoughts or feelings about the experiment.
 174

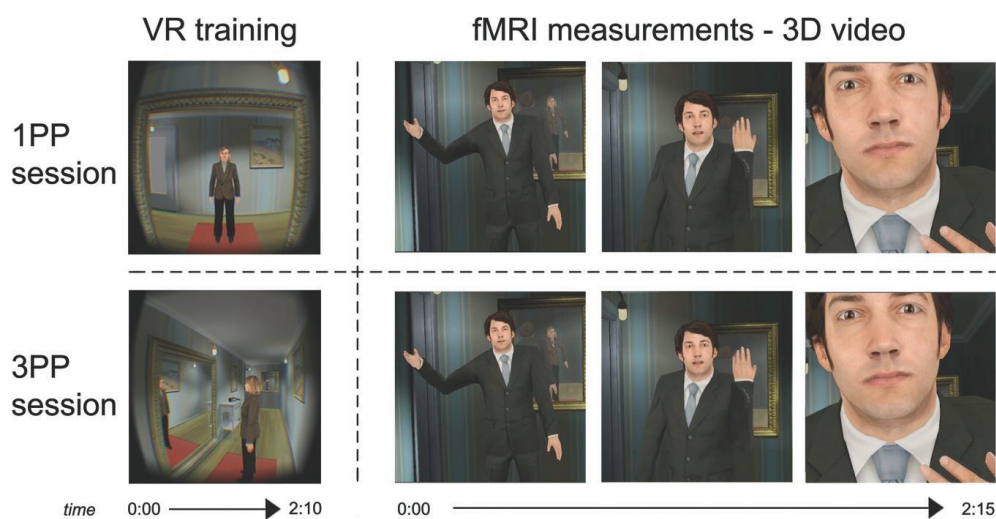


Fig. 1. Experimental design. In two counterbalanced sessions, participants were immersed in a virtual reality scenario (VR exposure) where they either observed the scenario from a first person perspective and performed visuomotor exercises congruent with the female character's movements (1PP; top left), or observed the scenario from a third person perspective and performed visuomotor exercises congruent with the virtual camera's movements (3PP; bottom left). In both sessions, participants were subsequently moved to an MRI scanner, where they watched a continuous 3D video showing a domestic violence situation in which a male aggressor approached the viewer and entered their personal space (right).

175

176 After a week, participants came back to the lab and followed the same procedure as during the first
177 session, but during this second session they viewed the VR scenario from the other perspective (e.g. if
178 they viewed it from third person perspective in the first session, then they viewed it from the first
179 person perspective in the second session). All other aspects of the session were identical. They also filled
180 out the VR questionnaire again at the end of the session and were debriefed about the contents and
181 meaning of the study. Again, the emotional state of the participants was assessed and they were asked
182 to contact the experimenter if they had any reoccurring thoughts or feelings, or were otherwise affected
183 by participating in this experiment. No participant reported to be distressed by the experiment or have
184 persisting thoughts or feelings about the experiment.

185

186 **Design**

187 The order of the VR exposure perspective (1PP vs. 3PP) between sessions was counterbalanced across
188 participants, so that half of the males and half of the females had the session order 1PP-3PP and the
189 other halves had the opposite order. The 3D video that was watched during fMRI measurements was
190 identical in both sessions and was preceded and followed by 3 seconds of fixation. The two experimental
191 conditions were the perception of the 3D video preceded by 1PP VR exposure (1PP session) and the
192 perception of the 3D video preceded by 3PP VR exposure (3PP session). The 3D stimulus was shown
193 once in each session, similar to other naturalistic research (e.g. Hasson et al., 2004).

194

195 **Data acquisition**

196 A 3T Siemens MR scanner (MAGNETOM Prisma, Siemens Medical Systems, Erlangen, Germany) with a
197 64 channel head/neck coil was used for imaging. Functional scans were acquired with a multiband
198 gradient echo echo-planar imaging sequence with a Repetition Time (TR) of 1500 milliseconds (ms) and
199 an Echo Time (TE) of 30 ms. The functional run consisted of 90 volumes comprising 57 slices (matrix =

200 100×100, 2 mm isotropic voxels, inter slice time = 26 ms, flip angle = 77°, multiband factor = 3, iPAT = 2).
201 After the functional run, high resolution T1-weighted structural images of the whole brain were acquired
202 with an MPRAGE with a TR of 2250 ms and a TE of 2.21 ms, 192 slices (matrix = 256×256, 1 mm isotropic
203 voxels, flip angle = 9°).

204

205 **Statistical analyses**

206 *Questionnaire analyses*

207 The VR questionnaire contained questions relating to the subjective experience of the 3D domestic
208 violence scenario. The scores on the VR questionnaire were compared between sessions (1PP vs. 3PP
209 priming) by conducting an Wilcoxon Signed Rank test (two-tailed), corrected for multiple comparisons
210 using a False Discovery Rate (FDR) of 0.05 (Benjamini and Hochberg, 1995). The significant results are
211 shown in Fig. 3. From the VR experience questionnaire, we used the scores on the question “To what
212 extent did you feel in the female body and lived the situation as if you were the woman?”, the question
213 “To what extent did you feel identified with the female body during the experience?” and the question
214 “To what extent have you experienced the situation as if it was real?” to analyze, respectively, the
215 perceived Body Ownership, Identification and Plausibility during the perception of the domestic violence
216 scenario.

217

218 *Functional MRI pre-processing*

219 The fMRI data were pre-processed and visualized using fMRI analysis and visualization software
220 BrainVoyager QX version 2.8.4 (Brain Innovation B.V., Maastricht, the Netherlands). Functional data
221 were corrected for head motion (3D motion correction, sinc interpolation), corrected for slice scan time
222 differences and temporally filtered (high pass, GLM-Fourier, 2 sines/cosines). For the ISC analyses, it is
223 recommended to spatially smooth the functional data with a Gaussian smoothing kernel of slightly

224 larger than double the original voxel size (Pajula and Tohka, 2014). Therefore, the functional data was
225 spatially smoothed using a Gaussian kernel with a FWHM of 5 mm. The anatomical data were corrected
226 for intensity inhomogeneity (Goebel et al., 2006) and transformed into Talairach space (Talairach and
227 Tournoux, 1988). The functional data were then aligned with the anatomical data and transformed into
228 the same space to create 4D volume time-courses (VTCs).

229

230 Head motion was below 1.1 mm for every participant (voxel size = 2 mm). We calculated the frame-wise
231 displacement (FWD; Power et al., 2012) for every participant in each session and compared the FWD
232 between sessions using a paired t-test, corrected for multiple comparisons using a FDR of 0.05, to
233 ensure that head motion did not differ between sessions. We found no differences in FWD between
234 conditions at any time point (FDR > 0.8). Out of all runs of the 1PP session (20 participants * 1 session)
235 90% of runs had 98.9% of time points with a FWD under 0.5 mm (Power et al., 2012). Out of all runs of
236 the 3PP session (20 participants * 1 session) also 90% of runs had 98.9% of time points with a FWD
237 under 0.5 mm. We also calculated the mean FWD across time points for each participant and compared
238 this between sessions using a paired t-test. We found no difference between sessions for the mean FWD
239 ($t(19) = -0.1212$, $p = 0.9048$). For all participants and sessions the mean FWD was below 0.5 mm
240 (maximum = 0.2 mm). The grand mean FWD (mean across participants and time points) was 0.0962 for
241 the 1PP session and 0.0958 for the 3PP session.

242

243 *Anatomical mask*

244 For the connectivity analyses and the second set of ISC analyses (see below), we defined anatomical
245 regions-of-interest (ROIs), which included regions relevant for perspective taking, embodiment,
246 peripersonal space, and emotion processing, as well as the primary auditory and visual cortex (see Table
247 1). Statistical Parametric Mapping (SPM; version 12, Functional Imaging Laboratory, London, UK) was

248 used to extract probabilistic cytoarchitectonic maps from the SPM Anatomy Toolbox (version 1.8,
 249 Forschungszentrum Jülich GmbH; Eickhoff et al., 2005). For regions that were not included in the
 250 Anatomy Toolbox we used the Hammers Adult maximum probability atlases (Hammers et al., 2003).

251

252 Table 1. Mean Talairach coordinates and cluster sizes of the regions of interest that were defined on the basis of anatomical
 253 probability atlases and used in the intersubject correlation and granger causality analysis.

Name	Hemisphere	Cluster size	Mean Talairach coordinates		
			X	y	z
Premotor cortex	Left	91529	-30	-12	44
	Right	91242	28	-15	44
Intraparietal sulcus	Left	38404	-35	-52	38
	Right	40746	36	-53	39
Primary somatosensory cortex	Left	85135	-32	-26	43
	Right	93873	31	-29	43
Supramarginal gyrus	Left	68995	-44	-37	33
	Right	70282	42	-39	32
Primary visual cortex	Left	36337	-13	-81	1
	Right	35727	14	-77	2
Primary auditory cortex	Left	13410	-45	-20	11
	Right	10218	46	-17	10
V5/MT	Left	6530	-41	-69	2
	Right	6685	46	-64	0
Superior parietal lobe	Left	78210	-18	-58	46
	Right	69199	18	-57	48
Amygdala	Left	5169	-22	-4	-13
	Right	5326	21	-5	-13
Anterior cingulate cortex	Left	23304	-7	20	31
	Right	28025	5	21	31
Anterior insula	Left	16817	-31	8	11
	Right	17361	29	8	10

254

255 Each voxel in a probabilistic region reflects the cytoarchitectonic probability (10–100%) of belonging to
 256 that region. We followed a procedure to obtain maximum probability maps as described in Eickhoff et
 257 al. (2006), as these are thought to provide ROIs that best reflect the anatomical hypotheses. This meant
 258 that all voxels in the ROI that were assigned to a certain area were set to “1” and the rest of the voxels
 259 were set to “0”. The ROIs were transformed from MNI space to Talairach space (as Talairach space was

260 used in the other analyses). We extracted the Colin27 anatomical data to help verify the subsequent
261 transformations. In order to transform the ROIs and the anatomical data from MNI space to Talairach
262 space, we imported the ANALYZE files in BrainVoyager, flipped the x-axis to set the data to radiological
263 format, and rotated the data -90° in the x-axis and $+90^\circ$ in the y-axis to get a sagittal orientation.
264 Subsequently, we transformed the Colin27 anatomical data to Talairach space (Talairach and Tournoux,
265 1988; Goebel et al., 2006) and applied the same transformations to the cytoarchitectonic ROIs. For the
266 ISC time course analysis on emotion processing (see section below and Fig. 7) we used the bilateral
267 probabilistic cytoarchitectonic maps of the AMG, anterior cingulate cortex (ACC) and the anterior
268 subdivision of the insula (aINS) as ROIs (excluding the middle and posterior subdivisions of the insula).

269

270 *Intersubject correlation*

271 The ISC toolbox for fMRI in Matlab (Kauppi et al., 2014) and in-house Matlab scripts were used for ISC
272 analyses with Matlab version R2013b, 8.2.0.701 (The MathWorks Inc., Natick, USA). We calculated
273 group-level ISC maps and ISC difference maps to reveal significant differences between conditions as
274 described in Kauppi et al. (2014). Pearson's correlation coefficient was used to calculate voxel-wise
275 temporal correlations between the VTC time-courses (90 volumes) of all possible subject pairs ($N(N - 1)$
276 $/ 2$). The group-level ISC is the sum of these correlation coefficients divided by the number of subject
277 pairs. The ISC maps for each condition were corrected using an FDR of 0.001. The ISC difference maps
278 between the sessions were calculated as described in Kauppi et al. (2014, section 2.2.4). In the ISC
279 difference analyses a Fisher's z-transformation (ZPF; Fisher, 1915) was applied to each pairwise
280 correlation in each voxel. Subsequently, a sum ZPF statistic for the difference between the two
281 conditions (1PP and 3PP) was calculated over all subject pairs and tested against the null hypothesis that
282 each ZPF value comes from a distribution with zero mean (no difference between 1PP and 3PP) using
283 non-parametric permutation testing (as the stimuli in the two conditions may not be independent). The

284 null distribution was obtained by randomly flipping the sign of pairwise ZPF statistics before calculating
285 the sum ZPF statistic using 25000 permutations (see Kauppi et al., 2014 for more details). Maximal and
286 minimal statistics over the entire image corresponding to each labeling were saved. The map was
287 thresholded at $\alpha = 0.05$ using the permutation distribution of maximal statistic, which accounts for the
288 multiple comparisons problem by controlling the FWER (see Nichols and Holmes, 2002).

289

290 In a second set of analyses we correlated the time course of the ISC in emotion processing regions with a
291 predictor that coded for aggressor proximity in order to understand whether emotion-related brain
292 activity becomes more synchronized across participants with approaching threat. In order to obtain the
293 time course of the ISC in each condition we calculated the average ISC in eight non-overlapping time
294 windows in three emotion-relevant ROIs (AMG, ACC, aINS). The first two volumes of the time courses
295 were excluded and the remaining 88 volumes were separated in eight time windows of 10 volumes,
296 which were each separate by 1 volume. Although short time windows could result in less reliable
297 estimates, the minimal window length depends on the stimulus and sample size. Windows of 10
298 samples have been used previously with 16 participants (Nummenmaa et al., 2012). Our approach
299 resulted in group-level ISC maps for each of the eight time windows per condition and ROI, reflecting the
300 moment-to-moment degree of intersubject synchronization across participants (Kauppi et al., 2014,
301 section 2.21). Subsequently, the voxel-wise correlation coefficients for all possible subject pairs were
302 transformed to z-scores using a Fisher's z transformation and the mean across all subject pairs was
303 calculated by summing the z-transformed correlation coefficients and dividing by the number of subject
304 pairs (Kauppi et al., 2014, section 2.2.3)). The mean across all voxels of an ROI was calculated for each of
305 the 8 maps, resulting in a mean time course of ISC with 8 time points (1 per time window) for each ROI
306 and condition. The resulting time courses were correlated with a predictor that coded for the position of
307 the aggressor in the 3D space during the course of the scenario. This predictor consisted of a box-car

308 function with “0” for the first 4 time windows that corresponded to the time during which the aggressor
309 was in far space (approximately two meters distance), and “1” for the remaining 4 time windows that
310 corresponded to the time during which the aggressor was in nearby space (approximately 30
311 centimeters distance) (see Fig. 2). The correlation coefficients were tested against the null hypothesis
312 that there is no relationship between the observed phenomena ($df = 6$). The results were corrected for
313 multiple comparisons using an FDR of 0.05 (Fig. 7).
314



Fig. 2. Visualization of the threat proximity predictor.

315

316 *Granger Causality Mapping*

317 We used the RFX GCM plugin of BrainVoyager QX 2.8 and in-house Matlab scripts to calculate effective
318 connectivity between brain regions. Granger Causality Mapping (GCM) (Roebroeck et al., 2005) uses
319 vector autoregressive models of fMRI time-series in the context of Granger causality. A time-series of
320 voxel X Granger causes a time-series of voxel Y, if the past of X improves the prediction of the current
321 value of Y, given that all other relevant sources of influence have been taken into account (including the
322 past of Y). As we had few hypotheses about the directions of connectivity between regions, we choose
323 to use GCM because it does not require a-priori modeling of the connectivity. Given the large amount of
324 regions included in our network, it did not seem feasible to map all possible connections, which would
325 be required for other approaches, such as dynamic causal modeling. We obtained whole-brain maps of
326 directed influence (dGCM) per session for each of the ROIs (Table 1) in each individual participant ($N =$
327 20), i.e. each region served as a reference region. These dGCM maps are maps with an influence

328 difference term for each voxel that has a positive value where influence from the reference region
329 dominates and a negative value where influence to the reference region dominates (Roebroek et al.,
330 2005). The individual dGCM maps were corrected for multiple comparisons using an FDR of 0.01. For
331 each reference region the 40 individual dGCM maps (20 participants, 2 sessions) with the influence
332 difference statistics were subsequently used in a second level RFX group analysis to calculate differences
333 in directed connectivity between conditions. For the group analysis a RFX ANOVA, with condition (1PP vs
334 3PP) as a within-subjects factor, was calculated for each reference region. The resulting whole-brain F-
335 maps were corrected for multiple comparisons using the cluster level statistical threshold estimator
336 plugin of BrainVoyager QX 2.8 (Goebel et al., 2006) with an initial threshold of $p = 0.005$ and a cluster
337 size corrected threshold of $p < 0.05$. When a whole-brain F-map of a reference region showed a cluster
338 with a difference in connectivity between conditions in one of the other ROIs, a mask containing the
339 voxels belonging to the cluster was saved. We performed this procedure for the F-maps of all reference
340 regions (e.g. LHIPS_RHPreM.msk, LHIPS_LHSMG.msk; RHACC_LHACC.msk, RHACC_RHPAC.msk).
341 Subsequently in order to create Fig. 5, we calculated for each reference region the mean dGCM maps
342 across participants within each mask for the 1PP and 3PP conditions separately. For the condition that
343 showed the largest mean value (either positive – indicating influence from the reference region, or
344 negative – indicating influence to the reference region) we added an arrow to Fig. 5 in the
345 corresponding condition. In cases where we found within the same region one cluster with the largest
346 mean value in 1PP session and one cluster with the largest mean value in the 3PP session we added an
347 arrow to both sections of Fig. 5. In order to counteract a potential downfall of GCM - that directed
348 connections may reflect inherent hemodynamic differences between regions (Deshpande et al., 2010) –
349 we compared effective connectivity between two conditions in an identical set of regions. If there are
350 inherent hemodynamic differences between regions, which give rise to false connections, these would

351 be present in both conditions. By only taking into account differences in connections between
352 conditions we circumvent the above mentioned problem.

353

354 In a second set of analyses we calculated the functional connectivity between regions for both
355 conditions using instantaneous GCM (correlation). Functional connectivity between two time-series X
356 and Y exists when the values of time-series X enhance predictions of contemporaneous values of the
357 time-series Y, taking into account other sources of influence (past X and Y) (Roebroeck et al., 2005).
358 Similar to the first set of dGCM analyses, we obtained whole-brain maps of instantaneous correlations
359 per session for each of the ROIs (see Table 1) in each individual participant (N = 20), i.e. each region
360 served as a reference region. For each reference region the 40 individual instantaneous GCM maps (20
361 participants, 2 sessions) were subsequently used in a second level RFX group analysis to calculate
362 differences in functional connectivity between conditions. For the group analysis a RFX ANOVA, with
363 condition (1PP vs 3PP) as a within-subjects factor, was calculated for each reference region. The
364 resulting whole-brain F-maps were corrected for multiple comparisons using the cluster level statistical
365 threshold estimator plugin of BrainVoyager QX 2.8 (Goebel et al., 2006) with an initial threshold of $p =$
366 0.005 and a cluster size corrected threshold of $p < 0.05$. The results are shown in Fig. 6.

367

368

369

370 **Results**371 **Subjective experience of perspective**

372 We assessed how participants experienced the virtual reality scenario by analyzing the VR
 373 questionnaires that were administrated at the end of each session. All questions were scored on a 1
 374 (Not at all) to 7 (Completely) Likert scale. The differences in answer scores between first and third
 375 person perspective conditions were analyzed using Wilcoxon Signed Rank test, corrected for multiple
 376 comparisons at FDR = 0.05 (see Methods section). Our main questions of interest related to differences
 377 in perceived Body Ownership, Identification and Plausibility. We found that participants reported higher
 378 Body Ownership and Identification during the VR threat scenario in the MRI scanner (Fig. 3) when they
 379 were previously exposed to first person perspective combined with visuo-motor exercises that were
 380 synchronous with the virtual body than when they were exposed to third person perspective combined
 381 with visuo-motor exercises without a virtual body.

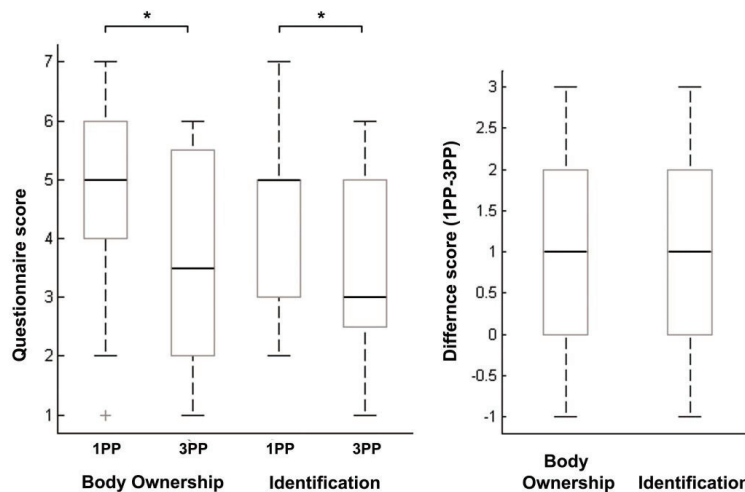


Fig. 3. Boxplots of VR questionnaire data. Left: The boxplots show the medians, interquartile ranges, maximum and minimum (as indicated by the stems) and outliers of the questionnaire scores that addressed the subjective experience of Body Ownership and Identification for each condition (1PP, 3PP). An asterisk indicates a significant difference (FDR < 0.05). Right: The boxplots show the medians, interquartile ranges, maximum and minimum of the difference scores (1PP-3PP) for Body Ownership and Identification.

382

383 Identification was assessed with question 1: “To what extent did you feel identified with the female
384 body during the experience?”. The results of the Wilcoxon Signed Rank test showed a significant
385 difference between conditions (FDR = 0.03), with higher scores of Identification in the 1PP session (1PP:
386 4.45 ± 0.33 ; 3PP: 3.50 ± 0.30) (Fig. 3, Left). Body ownership was assessed with question 2: “To what
387 extent did you feel in the female body and lived the situation as if you were the woman?”. The results of
388 the Wilcoxon Signed Rank test (Fig 2B) showed a significant difference between conditions (FDR = 0.04),
389 with higher scores of Body Ownership in the 1PP session (1PP: 4.85 ± 0.37 ; 3PP: 3.75 ± 0.39) (Fig. 3,
390 Left). Plausibility was assessed with question 3 “To what extent have you experienced the situation as if
391 it was real?”. The results of the Wilcoxon Signed Rank test did not show a significant difference between
392 sessions, but did show a trend for higher scores in the 1PP session compared to the 3PP session (1PP:
393 4.70 ± 0.36 ; 3PP: 3.70 ± 0.32 ; FDR = 0.05). No other item of the VR questionnaire showed a significant
394 difference between the conditions. Two items showed a trend for higher scores in the 1PP session
395 compared to the 3PP session. This was question 12.3 “To what extent did you find the following
396 behaviors of the male avatar threatening - When he invades your peri personal space and moves his
397 hands?” (1PP: 5.75 ± 0.31 ; 3PP: 4.90 ± 0.29 ; FDR = 0.05) and question 15 “Did you feel that the virtual
398 man was speaking and addressing to you personally?” (1PP: 4.05 ± 0.36 ; 3PP: 3.30 ± 0.33 ; FDR = 0.05).

399

400 **FMRI Approach**

401 In this study we wanted to explore perspective taking in the context of social threat in a naturalistic
402 manner. Therefore, we prioritized having two sessions with one continuous stimulus rather than a more
403 conventional approach with repeated presentation of different stimulus conditions in one session. The
404 nature of our complex stimulus meant that we could not use conventional analysis methods, such as the
405 GLM. Instead, we used ISC (Hasson et al., 2004) to compare spatiotemporal activity across participants
406 during the course of the natural stimulus perception. In this manner, we could identify stimulus-locked

407 neural responses across brains. In ISC analysis, the shared neural processing of participants is defined by
 408 calculating the correlation coefficient between fMRI time-series of participants in locations across the
 409 brain (see Methods). This makes ISC particularly suitable for naturalistic stimuli, such as 3D video, as it
 410 does not require modelling of the stimuli (Hasson et al., 2004; Hasson et al., 2008; Nummenmaa et al.,
 411 2012). After calculating an ISC map for each condition, we calculated ISC difference maps, which show
 412 the statistical difference between conditions in each voxel.

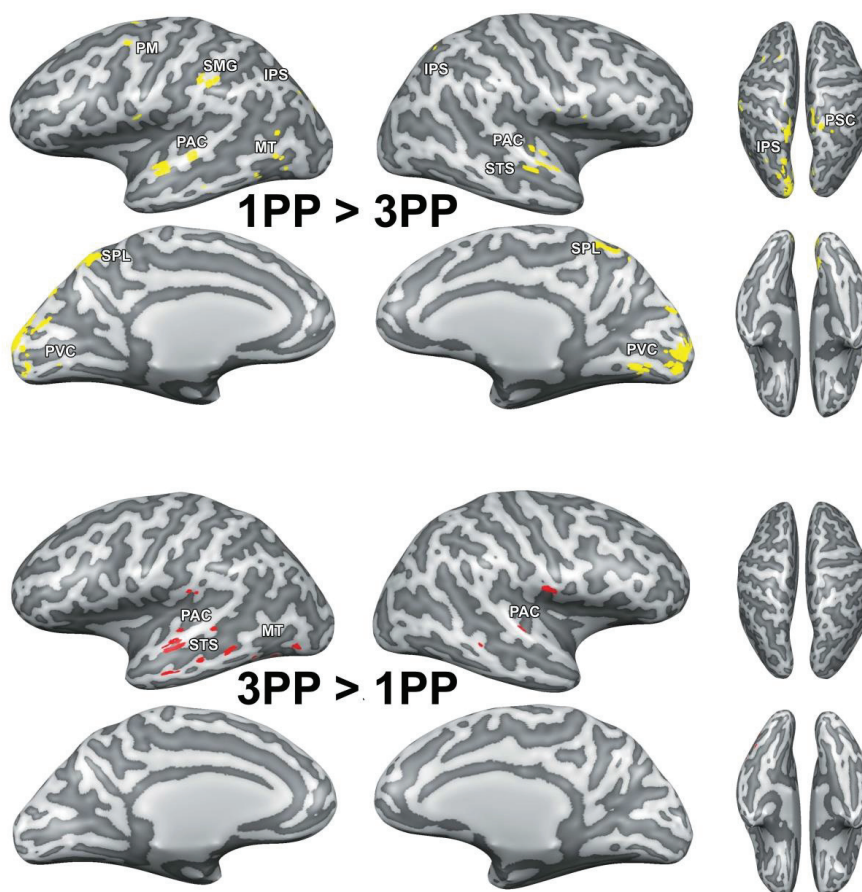


Fig. 4. Intersubject correlation differences (permutation testing, $N = 20$, $p[\text{corrected}] < 0.05$) between perception of an identical 3D domestic violence video preceded by first (1PP) and third person perspective (3PP) exposure. Voxels that showed significantly higher ISC after 1PP exposure than 3PP exposure are indicated in yellow (top). Voxels that showed significantly higher ISC after 3PP exposure than 1PP exposure are indicated in red (bottom). PAC = primary auditory cortex, PM = premotor cortex, SMG = supramarginal gyrus, MT = middle temporal area, SPL = superior parietal lobe, PVC = primary visual cortex, IPS = intraparietal sulcus, PSC = primary somatosensory cortex, STS = superior temporal sulcus.

413

414 Fronto-parietal network involved during first person perspective induced threat perception

415 The results of the fMRI analyses confirmed our first hypothesis: the multisensory network related to first
416 person perspective, body ownership and peripersonal space representation was more strongly
417 synchronized across participants after first than after third person perspective exposure. The ISC
418 difference maps (N = 20, p[FWER] < 0.05) showed that first person perspective exposure induced higher
419 ISC than third person perspective exposure in left dorsal and ventral PM, in bilateral IPS, left SMG,
420 bilateral SPL, right PSC and bilateral PVC during perception of the 3D video (Fig. 4, top). Additionally,
421 after both first (Fig. 4, top) and third person perspective exposure (Fig. 4, bottom) differences in ISC
422 were found in different areas of the bilateral PAC, superior temporal sulcus (STS) and left MT.

423

424 Virtual reality exposure influences effective connectivity in the fronto-parietal network

425 The results from the effective connectivity analyses did not confirm our second hypothesis – that visual
426 and somatosensory regions would send information to PM and IPS during first person embodied threat
427 perception. We calculated effective connectivity differences between the two conditions in an identical
428 set of regions using RFX ANCOVA analyses (see Methods, N = 20, p[corrected] < 0.05). We found that
429 during threat perception preceded by first person perspective exposure directed connections from PM,
430 IPS, SMG and MT towards SPL were stronger (see Fig. 5 top). This appears to suggest that information
431 was integrated in SPL. These findings are in line with the ISC results, which also emphasized changes in
432 these regions during the first person perspective session. Moreover, we found that bilateral PM showed
433 directed connections to many of the other regions in the network. Additionally, not shown in Fig. 5, we
434 found stronger directed connections from left PAC and left IPS to right ACC and from right ACC to right
435 AMG and left ACC after first person perspective exposure. Although we found that ISC was reduced in
436 the fronto-parietal network during third person perspective primed threat perception, the connectivity

437 results revealed a more complex situation (see Fig. 5 bottom). Contrary to the first person perspective
 438 session, we find stronger directed connectivity from IPS to PM, but information did not converge in
 439 posterior parietal cortex. Moreover, we found enhanced top-down connectivity from PM, IPS, SMG, SPL
 440 and PSC towards visual areas PVC and MT. Similarly, we also found that functional connectivity
 441 increased between PM, SMG, and SPL and the PVC in the 3PP session (Fig. 6). Additionally, not shown in
 442 Fig. 5, we found a directed connection from left SPL to right ACC after third person perspective
 443 exposure.
 444

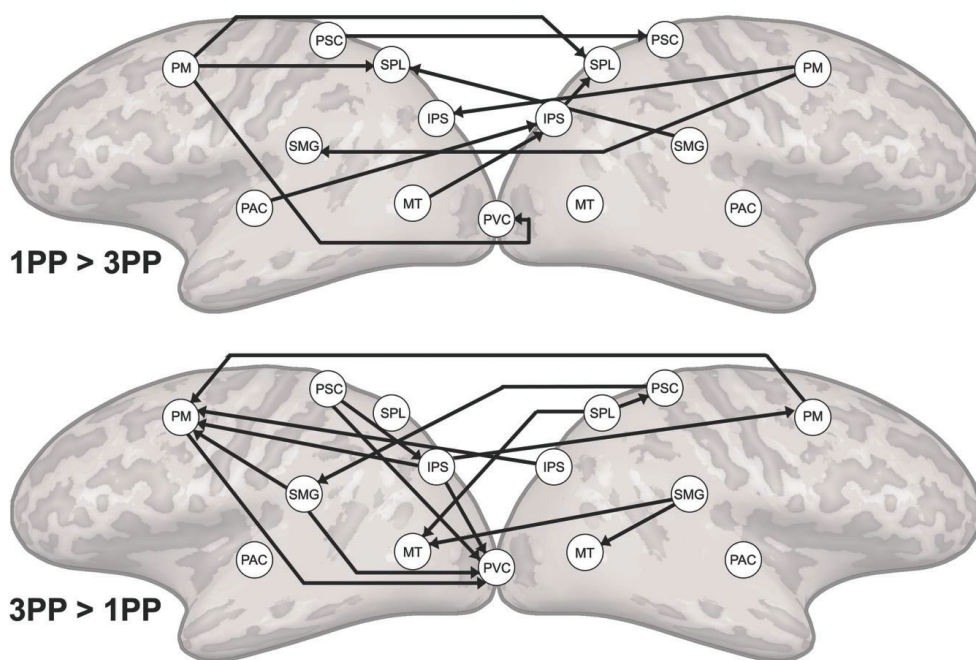


Fig. 5. Differences in effective connectivity between perception of an identical 3D threat video preceded by first (1PP) and third person perspective (3PP) exposure (RFX ANCOVA, $N = 20$, $p[\text{corrected}] < 0.05$). The arrows indicate the direction of the connectivity between regions that is unique for each condition. Abbreviations as in Fig. 4.

445

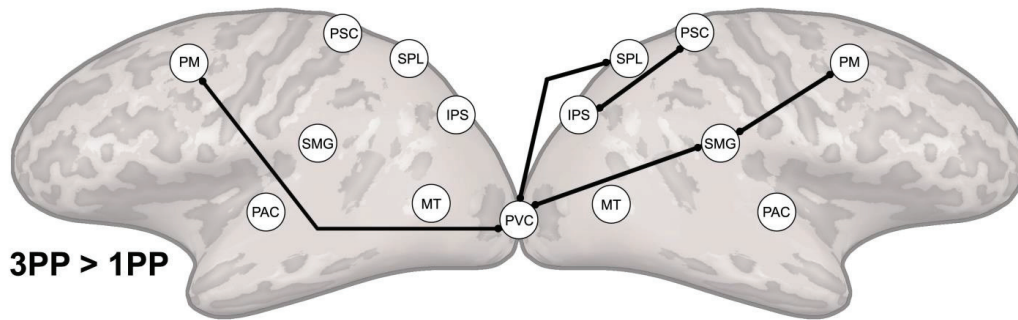


Fig. 6. Differences in functional connectivity between perception of an identical 3D threat video preceded by first (1PP) and third person perspective (3PP) exposure (RFX ANCOVA, $N = 20$, $p[\text{corrected}] < 0.05$). Abbreviations as in Fig. 4.

446

447 **Effect of first person perspective on threat processing in nearby space**

448 Finally, we investigated whether activity in emotion-related structures, such as AMG, is more strongly
 449 synchronized across participants when the participants had first person perspective embodied
 450 experience than third person perspective primed experience of nearby threat. Although we found no
 451 evidence for explicit experience of increased threat in the 1PP session in the questionnaire data, the
 452 trend ($FDR = 0.05$) for higher scores after first person perspective exposure found on question 12.3 “To
 453 what extent did you find the following behaviors of the male avatar threatening - when he invades your
 454 peri personal space and moves his hands?”, suggests that the intrusion into the personal space after first
 455 person perspective exposure may have had an effect on the consciously or subconsciously perceived
 456 threat. We calculated the time course of ISC in the ROIs of three emotion-related structures (bilateral
 457 AMG, ACC and aINS) using eight non-overlapping time windows of 10 volumes (see Methods).
 458 Subsequently, we correlated the time course of the ROI with a predictor that coded for threat proximity.
 459 We found (Fig. 7) that during the 1PP session the time course of ISC in the AMG significantly correlated
 460 with threat proximity ($R = 0.8062$, $FDR < 0.05$), while it did not in the 3PP session ($R = 0.1107$, $FDR > 0.9$).
 461 For the ACC and the aINS the ISC time courses did not correlate significantly with threat distance in the
 462 1PP session (ACC: $R = 0.5796$, $FDR > 0.1$; aINS: $R = 0.1078$, $FDR > 0.7$) and the 3PP session (ACC: $R =$

463 0.2607, $FDR > 0.9$; aINS: $R = -0.0443$, $FDR > 0.9$). These results indicate that when the participants were
464 embodied in the virtual victim after first person perspective exposure, the increased intersubject
465 synchronization of the AMG signaled the proximity of the aggressor, while this was not the case after
466 third person perspective exposure.

467

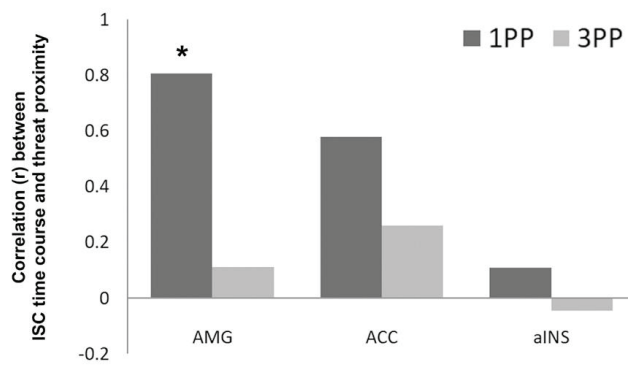


Fig. 7. Correlation between threat proximity and the intersubject correlation (ISC) time course within each region-of-interest in the 1PP (dark grey) and the 3PP (light grey) session. An asterisk indicates a significant relationship between threat proximity and ISC.

468

469

470 **Discussion**

471 **Influence of perspective exposure on fronto-parietal network**

472 Our first hypothesis was that synchronization of brain activity across participants in the fronto-parietal
473 network will be stronger when a threat is primed to be in our own space (first person perspective
474 embodied exposure) than in another's space (third person perspective exposure). The results of the ISC
475 analyses indicated a clear effect of first versus third person perspective exposure on the neural
476 synchronization in this network. After first person perspective exposure we found that all regions
477 related to body ownership and nearby space representation, including PM, IPS, SMG, SPL and PSC, were
478 more synchronized across participants. This was not the case when participants were exposed to a third
479 person perspective. We expected that during 1PP primed threat perception sensory information from
480 PVC, PAC, and PSC would converge via the IPS in the PM, as the PM should initiate the defensive
481 responses. We based this hypothesis on the fact that electrical stimulation of F4 and VIP in monkeys
482 (human homologues of superior vPM and ventral IPS) produces movements similar to defensive
483 movements followed by air puffs (Cooke and Graziano, 2003, 2004) and on the existing anatomical
484 connections from monkey VIP to F4 (Luppino et al., 1999). Research in humans also indicated the
485 involvement of PM in threat-related processing (Pichon et al., 2012). Therefore, the ventral PM-IPS
486 network is believed to function to protect the near personal space (Clery et al., 2015). Our findings do
487 indicate the involvement of superior ventral PM and IPS (Fig. 4), but show a convergence of information
488 in SPL rather than vPM in the 1PP session. The SPL is an area where many different cognitive functions
489 converge, including attention (Kastner et al., 1999), spatial imagery and perception (Ungerleider and
490 Haxby, 1994; Formisano et al., 2002; de Borst et al., 2012) and the generation and guidance of actions
491 (Culham and Kanwisher, 2001). The superior parietal cortex also underlies the transformation of
492 multisensory input to different coordinate systems, e.g. head, arm, body centered (Andersen et al.,
493 1993), and converting this information into motor commands and whole body actions to targets (Buneo

494 and Andersen, 2006; Whitlock et al., 2008). Together with the PM and IPS, the SPL may monitor, predict
495 and evade intrusive actions towards the body (Lloyd et al., 2006; Clery et al., 2015). Our results indicate
496 that these brain regions “tick together” across participants more strongly when participants are
497 embodied in the virtual victim of domestic abuse.

498

499 After third person perspective exposure we observed that brain activity in this fronto-parietal network
500 was not synchronized consistently across participants. We hypothesize that this may indicate that after
501 first person embodiment the body and nearby space representation is aligned with the virtual body and
502 intrusion of this space synchronizes activity across participants in the fronto-parietal network, while
503 after third person perspective exposure this does not occur. Indeed, our ISC findings suggest that
504 exposure to a third person perspective does not synchronize the personal space network and this aspect
505 of the results did not provide support for a shared peripersonal space that is independent of
506 perspective. However, the effective connectivity results did show third person perspective specific
507 modulations in the fronto-parietal network. We found an increase in connectivity from IPS to PM and an
508 increase of top-down connectivity from the peripersonal space network nodes (PM, IPS, SMG, PSC)
509 towards the primary visual areas and MT. The former results indicate that although information was
510 sent from IPS to PM in line with peripersonal space encoding models and existing anatomical
511 connections (Luppino et al., 1999), the ISC results showed that the underlying brain activity in these
512 regions was not very similar across participants. Nevertheless, these results do indicate a role for
513 peripersonal space representation even if the stimulus is perceived passively in the victim’s space,
514 perhaps for the protection of others. Moreover, we found that after 3PP exposure there was overall
515 more top-down connectivity to visual areas. The increased effective and functional connectivity
516 between PVC and IPS, SPL and SMG suggests that monitoring of the moving visual stimulus took place
517 after third person perspective exposure. Although the video that the participants viewed in the MRI

518 scanner was identical in both conditions, the top-down modulation of visual areas we observed here
519 may indicate that the imposed third person perspective altered spatial attention, similar to how task
520 differences can alter attention during identical stimulation (Li et al., 2004).

521

522 **Role of the temporoparietal cortex**

523 Previous research has shown that the temporoparietal cortex (including the temporoparietal junction
524 (TPJ) and SMG) is implied in perspective taking (Maguire et al., 1998; Ruby and Decety, 2001; Falk et al.,
525 2012; Besharati et al., 2016), interoception (Kashkouli Nejad et al., 2015) and self-other distinction
526 (Steinbeis et al., 2015). For example, viewing painful stimulation of a hand evoked activity in bilateral
527 SMG, which was linked to simulated pain to the own body (Costantini et al., 2008). The TPJ/SMG has
528 also been mentioned as part of the multisensory representation of peripersonal space (Lloyd et al.,
529 2003; Makin et al., 2007; Brozzoli et al., 2012; Grivaz et al., 2017). The results of our ISC analyses
530 indicated that the SMG is more strongly synchronized during threat perception preceded by first than
531 third person perspective exposure. However, the connectivity analyses indicate that the SMG was an
532 integrated part of the network in both conditions. In the 1PP session it received information from PM
533 and sent information to SPL, which is in line with anatomical connections between the SMG, ventral PM
534 and IPS in the human brain (Rushworth et al., 2006). In the 3PP session, the SMG send information to
535 visual areas and PM and was functionally connected with these regions as well. These results suggest
536 that the temporo-parietal cortex plays a more general role in perspective taking and relating body
537 relevant information to the self.

538

539 **Affective responses to first person experience of threat**

540 Our second hypothesis focused on synchronized brain activity in emotion-processing regions during first
541 person perspective experience of nearby threat. Threat monitoring and defensive responses are

542 especially enhanced when the threat is near, as shown by a series of experiments with virtual characters
543 (Ahs et al., 2015) and threatening stimuli (Mobbs et al., 2009; Mobbs et al., 2010; de Haan et al., 2016;
544 Wabnegger et al., 2016). A recent study showed that the AMG is more activated when moving from
545 threat anticipation to threat confrontation (Klumpers et al., 2017). Our results support these findings.
546 We found that brain activity is more synchronized across participants in the AMG when the stimulus was
547 perceived to be near the body (1PP condition). We found this effect only in the AMG, not in other
548 emotion-relevant structures such as the ACC and aINS. This further emphasizes the special role of the
549 amygdala in regulating interpersonal distance by signaling when stimuli come near the body (Kennedy et
550 al., 2009; Klumpers et al., 2017). We found no evidence for enhanced ISC in any of the emotion
551 processing regions when the stimulus was perceived as directed to another person. The findings of
552 subjective experience questionnaire indicated that the VR exposure from first person perspective was
553 effective in eliciting identification with the virtual victim and thereby may have enhanced
554 synchronization of (non-conscious) affective responses to nearby threat (in line with Galvan Debarba et
555 al., 2017). Although we found no direct evidence for increased experience of threat after first person
556 perspective exposure, previous research has shown that emotion processing often takes place on a non-
557 conscious level (Tamietto and de Gelder, 2010). We did find a trend for higher scores on the experience
558 of threat when the aggressor entered the peripersonal space after first person perspective exposure
559 (see Results), which is in line with the increased synchronization of brain activity across participants in
560 the AMG during this event.

561

562 In addition we found modulations of connectivity towards the emotion processing regions during the
563 perception of the scenario, both after first and third person perspective exposure. The connectivity
564 analyses revealed that in the first person perspective session PAC and IPS sent information to right ACC
565 and from the right ACC information was forwarded to right AMG and left ACC. The ACC has a general

566 role in decision making and social and emotional processing (Lavin et al., 2013) and has bilateral
567 connections to the premotor and auditory cortex (Jacobson and Trojanowski, 1977; Muller-Preuss et al.,
568 1980; Vogt and Pandya, 1987; Barbas, 1988; Petrides and Pandya, 1988; Barbas et al., 1999). Moreover,
569 the ACC is linked to vocalizations (Muller-Preuss and Ploog, 1981; Dolan et al., 1995; Frith and Dolan,
570 1996) and auditory processing of speech in humans (Paus et al., 1993; Frith et al., 1995) and is
571 connected to the limbic system, including the AMG. This link suggests a role of ACC in the appraisal and
572 regulating of emotions (Etkin et al., 2011) and in encoding emotional significance of auditory stimuli.

573

574 **Future directions**

575 In this study we found that VR exposure is particularly suitable for fMRI experiments. Our study
576 exemplifies how exposure of body ownership in VR outside of the MRI environment, in combination
577 with a 3D video during fMRI measurements, can greatly contribute to the possibilities of naturalistic
578 methodologies in social and affective neuroimaging experiments. The scarcity of human neuroscience
579 studies using dynamic threatening stimuli contrasts with the relevance of personal space intrusion in the
580 perception of threat, both for the victims (Lloyd et al., 2006) and for the aggressors (Schienle et al.,
581 2016). As static threatening stimuli may fail to evoke realistic responses, naturalistic immersive 3D
582 motion stimuli appear better suited to modulate the approach of threatening stimuli within a
583 naturalistic environment that the participants may perceive as real. Here we used a single short stimulus
584 preceded by two different types of VR exposure in order to isolate the effect of perspective, keep all
585 visual stimulus properties equal and maximize the perceived realism and emotional impact with only
586 one stimulus repetition. However, this does limit our findings to this specific stimulus and does not allow
587 for further disentangling of neural responses to emotional vs. neutral stimuli within nearby space.
588 Future studies may further variate the types of stimuli used and test whether synchronization of activity
589 in the fronto-parietal brain network is specific for emotional stimuli after first person perspective

590 exposure or applies to other types of stimuli as well. Another line of future study could relate to
591 potential gender differences in body ownership and threat experience. In this study, we embodied all
592 participants (male and female) in a female virtual character. For the female participants it may have
593 been easier to place themselves in the victims' shoes than for the male participants. Moreover, male
594 and female participants may respond differently to a male aggressor (Wabnegger et al., 2016). Future
595 work could design a study with a larger number of participants, as our study was underpowered to
596 perform gender specific analyses, and a simpler design, which would allow for disentangling possible
597 gender differences. Our study shows that first person perspective visuo-motor exercises in VR can be
598 utilized to prime subsequent experiences such that behavioral and neuronal responses are aligned with
599 the virtual victim. Combining immersive VR exposure with neuroimaging methods could provide a basis
600 for behavioral change during therapeutic treatment (Seinfeld et al., 2018).

601

602 **References**

- 603 Ahs F, Dunsmoor JE, Zielinski D, LaBar KS (2015) Spatial proximity amplifies valence in emotional
604 memory and defensive approach-avoidance. *Neuropsychologia* 70:476-485.
- 605 Andersen RA, Snyder LH, Li CS, Stricanne B (1993) Coordinate transformations in the representation of
606 spatial information. *Current opinion in neurobiology* 3:171-176.
- 607 Banakou D, Slater M (2014) Body ownership causes illusory self-attribution of speaking and influences
608 subsequent real speaking. *Proceedings of the National Academy of Sciences of the United States*
609 *of America* 111:17678-17683.
- 610 Banakou D, Groten R, Slater M (2013) Illusory ownership of a virtual child body causes overestimation of
611 object sizes and implicit attitude changes. *Proceedings of the National Academy of Sciences of*
612 *the United States of America* 110:12846-12851.
- 613 Barbas H (1988) Anatomic organization of basoventral and mediodorsal visual recipient prefrontal
614 regions in the rhesus monkey. *The Journal of comparative neurology* 276:313-342.
- 615 Barbas H, Ghashghaei H, Dombrowski SM, Rempel-Clower NL (1999) Medial prefrontal cortices are
616 unified by common connections with superior temporal cortices and distinguished by input from
617 memory-related areas in the rhesus monkey. *The Journal of comparative neurology* 410:343-
618 367.
- 619 Bartels A, Zeki S (2004) Functional brain mapping during free viewing of natural scenes. *Human brain*
620 *mapping* 21:75-85.
- 621 Benjamini Y, Hochberg Y (1995) Controlling the False Discovery Rate: A Practical and Powerful Approach
622 to Multiple Testing. *Journal of the Royal Statistical Society Series B (Methodological)* 57:289-300.
- 623 Besharati S, Forkel SJ, Kopelman M, Solms M, Jenkinson PM, Fotopoulou A (2016) Mentalizing the body:
624 spatial and social cognition in anosognosia for hemiplegia. *Brain : a journal of neurology*
625 139:971-985.
- 626 Blanke O (2012) Multisensory brain mechanisms of bodily self-consciousness. *Nature reviews*
627 *Neuroscience* 13:556-571.
- 628 Brozzoli C, Gentile G, Ehrsson HH (2012) That's near my hand! Parietal and premotor coding of hand-
629 centered space contributes to localization and self-attribution of the hand. *The Journal of*
630 *neuroscience : the official journal of the Society for Neuroscience* 32:14573-14582.
- 631 Buneo CA, Andersen RA (2006) The posterior parietal cortex: sensorimotor interface for the planning
632 and online control of visually guided movements. *Neuropsychologia* 44:2594-2606.
- 633 Clery J, Guipponi O, Wardak C, Ben Hamed S (2015) Neuronal bases of peripersonal and extrapersonal
634 spaces, their plasticity and their dynamics: knowns and unknowns. *Neuropsychologia* 70:313-
635 326.
- 636 Cooke DF, Graziano MS (2003) Defensive movements evoked by air puff in monkeys. *Journal of*
637 *neurophysiology* 90:3317-3329.
- 638 Cooke DF, Graziano MS (2004) Sensorimotor integration in the precentral gyrus: polysensory neurons
639 and defensive movements. *Journal of neurophysiology* 91:1648-1660.
- 640 Costantini M, Galati G, Romani GL, Aglioti SM (2008) Empathic neural reactivity to noxious stimuli
641 delivered to body parts and non-corporeal objects. *The European journal of neuroscience*
642 28:1222-1230.
- 643 Culham JC, Kanwisher NG (2001) Neuroimaging of cognitive functions in human parietal cortex. *Current*
644 *opinion in neurobiology* 11:157-163.
- 645 de Borst AW, Sack AT, Jansma BM, Esposito F, de Martino F, Valente G, Roebroek A, di Salle F, Goebel
646 R, Formisano E (2012) Integration of "what" and "where" in frontal cortex during visual imagery
647 of scenes. *NeuroImage* 60:47-58.

- 648 de Haan AM, Smit M, Van der Stigchel S, Dijkerman HC (2016) Approaching threat modulates
649 visuotactile interactions in peripersonal space. *Experimental brain research* 234:1875-1884.
- 650 Deshpande G, Sathian K, Hu X (2010) Effect of hemodynamic variability on Granger causality analysis of
651 fMRI. *Neuroimage* 52:884-896.
- 652 Dolan RJ, Fletcher P, Frith CD, Friston KJ, Frackowiak RS, Grasby PM (1995) Dopaminergic modulation of
653 impaired cognitive activation in the anterior cingulate cortex in schizophrenia. *Nature* 378:180-
654 182.
- 655 Ehrsson HH (2012) The concept of body ownership and its relation to multisensory integration. In: *The*
656 *new handbook of multisensory processing* (Stein BE, ed): MIT Press.
- 657 Ehrsson HH, Wiech K, Weiskopf N, Dolan RJ, Passingham RE (2007) Threatening a rubber hand that you
658 feel is yours elicits a cortical anxiety response. *Proceedings of the National Academy of Sciences*
659 *of the United States of America* 104:9828-9833.
- 660 Eickhoff SB, Heim S, Zilles K, Amunts K (2006) Testing anatomically specified hypotheses in functional
661 imaging using cytoarchitectonic maps. *NeuroImage* 32:570-582.
- 662 Eickhoff SB, Stephan KE, Mohlberg H, Grefkes C, Fink GR, Amunts K, Zilles K (2005) A new SPM toolbox
663 for combining probabilistic cytoarchitectonic maps and functional imaging data. *NeuroImage*
664 25:1325-1335.
- 665 Falk EB, Spunt RP, Lieberman MD (2012) Ascribing beliefs to ingroup and outgroup political candidates:
666 neural correlates of perspective-taking, issue importance and days until the election.
667 *Philosophical transactions of the Royal Society of London Series B, Biological sciences* 367:731-
668 743.
- 669 Fernandes O, Jr., Portugal LC, Alves RC, Arruda-Sanchez T, Rao A, Volchan E, Pereira M, Oliveira L,
670 Mourao-Miranda J (2016) Decoding negative affect personality trait from patterns of brain
671 activation to threat stimuli. *NeuroImage*.
- 672 Fisher RA (1915) Frequency Distribution of the Values of the Correlation Coefficient in Samples from an
673 Indefinitely Large Population. *Biometrika* 10:507-521.
- 674 Formisano E, Linden DE, Di Salle F, Trojano L, Esposito F, Sack AT, Grossi D, Zanella FE, Goebel R (2002)
675 Tracking the mind's image in the brain I: time-resolved fMRI during visuospatial mental imagery.
676 *Neuron* 35:185-194.
- 677 Frith C, Dolan R (1996) The role of the prefrontal cortex in higher cognitive functions. *Brain research*
678 *Cognitive brain research* 5:175-181.
- 679 Frith CD, Friston KJ, Herold S, Silbersweig D, Fletcher P, Cahill C, Dolan RJ, Frackowiak RS, Liddle PF
680 (1995) Regional brain activity in chronic schizophrenic patients during the performance of a
681 verbal fluency task. *The British journal of psychiatry : the journal of mental science* 167:343-349.
- 682 Galvan Debarba H, Bovet S, Salomon R, Blanke O, Herbelin B, Boulic R (2017) Characterizing first and
683 third person viewpoints and their alternation for embodied interaction in virtual reality. *PLoS*
684 *One* 12:e0190109.
- 685 Goebel R, Esposito F, Formisano E (2006) Analysis of functional image analysis contest (FIAC) data with
686 brainvoyager QX: From single-subject to cortically aligned group general linear model analysis
687 and self-organizing group independent component analysis. *Human brain mapping* 27:392-401.
- 688 Grivaz P, Blanke O, Serino A (2017) Common and distinct brain regions processing multisensory bodily
689 signals for peripersonal space and body ownership. *NeuroImage* 147:602-618.
- 690 Hamilton-Giachritsis C, Banakou D, Garcia Quiroga M, Giachritsis C, Slater M (2018) Reducing risk and
691 improving maternal perspective-taking and empathy using virtual embodiment. *Sci Rep* 8:2975.
- 692 Hammers A, Allom R, Koepp MJ, Free SL, Myers R, Lemieux L, Mitchell TN, Brooks DJ, Duncan JS (2003)
693 Three-dimensional maximum probability atlas of the human brain, with particular reference to
694 the temporal lobe. *Hum Brain Mapp* 19:224-247.

- 695 Han S, Gao X, Humphreys GW, Ge J (2008) Neural processing of threat cues in social environments.
696 Human brain mapping 29:945-957.
- 697 Hasson U, Nir Y, Levy I, Fuhrmann G, Malach R (2004) Intersubject synchronization of cortical activity
698 during natural vision. *Science* 303:1634-1640.
- 699 Hasson U, Furman O, Clark D, Dudai Y, Davachi L (2008) Enhanced intersubject correlations during movie
700 viewing correlate with successful episodic encoding. *Neuron* 57:452-462.
- 701 Jacobson S, Trojanowski JQ (1977) Prefrontal granular cortex of the rhesus monkey. I. Intrahemispheric
702 cortical afferents. *Brain research* 132:209-233.
- 703 Kashkouli Nejad K, Sugiura M, Nozawa T, Kotozaki Y, Furusawa Y, Nishino K, Nukiwa T, Kawashima R
704 (2015) Supramarginal activity in interoceptive attention tasks. *Neuroscience letters* 589:42-46.
- 705 Kastner S, Pinsk MA, De Weerd P, Desimone R, Ungerleider LG (1999) Increased activity in human visual
706 cortex during directed attention in the absence of visual stimulation. *Neuron* 22:751-761.
- 707 Kauppi JP, Pajula J, Tohka J (2014) A versatile software package for inter-subject correlation based
708 analyses of fMRI. *Frontiers in neuroinformatics* 8:2.
- 709 Kennedy DP, Glascher J, Tyszka JM, Adolphs R (2009) Personal space regulation by the human amygdala.
710 *Nat Neurosci* 12:1226-1227.
- 711 Klumpers F, Kroes MCW, Baas J, Fernandez G (2017) How human amygdala and bed nucleus of the stria
712 terminalis may drive distinct defensive responses. *The Journal of neuroscience : the official*
713 *journal of the Society for Neuroscience*.
- 714 Kokkinara E, Slater M (2014) Measuring the effects through time of the influence of visuomotor and
715 visuotactile synchronous stimulation on a virtual body ownership illusion. *Perception* 43:43-58.
- 716 Lavin C, Melis C, Mikulan E, Gelormini C, Huepe D, Ibanez A (2013) The anterior cingulate cortex: an
717 integrative hub for human socially-driven interactions. *Frontiers in neuroscience* 7:64.
- 718 LeDoux J (2003) The emotional brain, fear, and the amygdala. *Cell Mol Neurobiol* 23:727-738.
- 719 Li W, Piech V, Gilbert CD (2004) Perceptual learning and top-down influences in primary visual cortex.
720 *Nature neuroscience* 7:651-657.
- 721 Lloyd D, Morrison I, Roberts N (2006) Role for human posterior parietal cortex in visual processing of
722 aversive objects in peripersonal space. *Journal of neurophysiology* 95:205-214.
- 723 Lloyd DM, Shore DI, Spence C, Calvert GA (2003) Multisensory representation of limb position in human
724 premotor cortex. *Nature neuroscience* 6:17-18.
- 725 Luppino G, Murata A, Govoni P, Matelli M (1999) Largely segregated parietofrontal connections linking
726 rostral intraparietal cortex (areas AIP and VIP) and the ventral premotor cortex (areas F5 and
727 F4). *Exp Brain Res* 128:181-187.
- 728 Maguire EA, Burgess N, Donnett JG, Frackowiak RS, Frith CD, O'Keefe J (1998) Knowing where and
729 getting there: a human navigation network. *Science* 280:921-924.
- 730 Maister L, Slater M, Sanchez-Vives MV, Tsakiris M (2015) Changing bodies changes minds: owning
731 another body affects social cognition. *Trends in cognitive sciences* 19:6-12.
- 732 Makin TR, Holmes NP, Zohary E (2007) Is that near my hand? Multisensory representation of
733 peripersonal space in human intraparietal sulcus. *The Journal of neuroscience : the official*
734 *journal of the Society for Neuroscience* 27:731-740.
- 735 Mobbs D, Yu R, Rowe JB, Eich H, FeldmanHall O, Dalgleish T (2010) Neural activity associated with
736 monitoring the oscillating threat value of a tarantula. *Proceedings of the National Academy of*
737 *Sciences of the United States of America* 107:20582-20586.
- 738 Mobbs D, Marchant JL, Hassabis D, Seymour B, Tan G, Gray M, Petrovic P, Dolan RJ, Frith CD (2009) From
739 threat to fear: the neural organization of defensive fear systems in humans. *The Journal of*
740 *neuroscience : the official journal of the Society for Neuroscience* 29:12236-12243.
- 741 Muller-Preuss P, Ploog D (1981) Inhibition of auditory cortical neurons during phonation. *Brain research*
742 215:61-76.

- 743 Muller-Preuss P, Newman JD, Jurgens U (1980) Anatomical and physiological evidence for a relationship
744 between the 'cingular' vocalization area and the auditory cortex in the squirrel monkey. *Brain*
745 *research* 202:307-315.
- 746 Nichols TE, Holmes AP (2002) Nonparametric permutation tests for functional neuroimaging: a primer
747 with examples. *Human brain mapping* 15:1-25.
- 748 Nummenmaa L, Glerean E, Viinikainen M, Jaaskelainen IP, Hari R, Sams M (2012) Emotions promote
749 social interaction by synchronizing brain activity across individuals. *Proceedings of the National*
750 *Academy of Sciences of the United States of America* 109:9599-9604.
- 751 Pajula J, Tohka J (2014) Effects of spatial smoothing on inter-subject correlation based analysis of fMRI.
752 *Magnetic resonance imaging* 32:1114-1124.
- 753 Paus T, Petrides M, Evans AC, Meyer E (1993) Role of the human anterior cingulate cortex in the control
754 of oculomotor, manual, and speech responses: a positron emission tomography study. *Journal*
755 *of neurophysiology* 70:453-469.
- 756 Pereira AG, Moita MA (2016) Is there anybody out there? Neural circuits of threat detection in
757 vertebrates. *Curr Opin Neurobiol* 41:179-187.
- 758 Petrides M, Pandya DN (1988) Association fiber pathways to the frontal cortex from the superior
759 temporal region in the rhesus monkey. *The Journal of comparative neurology* 273:52-66.
- 760 Pichon S, de Gelder B, Grezes J (2012) Threat prompts defensive brain responses independently of
761 attentional control. *Cerebral cortex* 22:274-285.
- 762 Power JD, Barnes KA, Snyder AZ, Schlaggar BL, Petersen SE (2012) Spurious but systematic correlations
763 in functional connectivity MRI networks arise from subject motion. *Neuroimage* 59:2142-2154.
- 764 Rizzolatti G, Scandolaria C, Matelli M, Gentilucci M (1981) Afferent properties of periarculate neurons in
765 macaque monkeys. II. Visual responses. *Behavioural brain research* 2:147-163.
- 766 Roebroeck A, Formisano E, Goebel R (2005) Mapping directed influence over the brain using Granger
767 causality and fMRI. *NeuroImage* 25:230-242.
- 768 Ruby P, Decety J (2001) Effect of subjective perspective taking during simulation of action: a PET
769 investigation of agency. *Nature neuroscience* 4:546-550.
- 770 Rushworth MF, Behrens TE, Johansen-Berg H (2006) Connection patterns distinguish 3 regions of human
771 parietal cortex. *Cereb Cortex* 16:1418-1430.
- 772 Schienle A, Wabnegger A, Leitner M, Leutgeb V (2016) Neuronal correlates of personal space intrusion in
773 violent offenders. *Brain imaging and behavior*.
- 774 Seinfeld S, Arroyo-Palacios J, Iruretagoyena G, Hortensius R, Zapata LE, Borland D, de Gelder B, Slater M,
775 Sanchez-Vives MV (2018) Offenders become the victim in virtual reality: impact of changing
776 perspective in domestic violence. *Sci Rep* 8:2692.
- 777 Serino A (2019) Peripersonal space (PPS) as a multisensory interface between the individual and the
778 environment, defining the space of the self. *Neurosci Biobehav Rev* 99:138-159.
- 779 Silva BA, Gross CT, Graff J (2016) The neural circuits of innate fear: detection, integration, action, and
780 memorization. *Learn Mem* 23:544-555.
- 781 Slater M (2009) Place illusion and plausibility can lead to realistic behaviour in immersive virtual
782 environments. *Philosophical transactions of the Royal Society of London Series B, Biological*
783 *sciences* 364:3549-3557.
- 784 Steinbeis N, Bernhardt BC, Singer T (2015) Age-related differences in function and structure of rSMG and
785 reduced functional connectivity with DLPFC explains heightened emotional egocentricity bias in
786 childhood. *Social cognitive and affective neuroscience* 10:302-310.
- 787 Sussman TJ, Jin J, Mohanty A (2016) Top-down and bottom-up factors in threat-related perception and
788 attention in anxiety. *Biol Psychol* 121:160-172.
- 789 Talairach J, Tournoux P (1988) Co-planar stereotaxic atlas of the human brain : 3-dimensional
790 proportional system : an approach to medical cerebral imaging. New York: Thieme.

- 791 Tamietto M, de Gelder B (2010) Neural bases of the non-conscious perception of emotional signals. *Nat*
792 *Rev Neurosci* 11:697-709.
- 793 Ungerleider LG, Haxby JV (1994) 'What' and 'where' in the human brain. *Current opinion in neurobiology*
794 4:157-165.
- 795 Vogt BA, Pandya DN (1987) Cingulate cortex of the rhesus monkey: II. Cortical afferents. *The Journal of*
796 *comparative neurology* 262:271-289.
- 797 Wabnegger A, Leutgeb V, Schienle A (2016) Differential amygdala activation during simulated personal
798 space intrusion by men and women. *Neuroscience* 330:12-16.
- 799 Whitlock JR, Sutherland RJ, Witter MP, Moser MB, Moser EI (2008) Navigating from hippocampus to
800 parietal cortex. *Proceedings of the National Academy of Sciences of the United States of*
801 *America* 105:14755-14762.
- 802